European Journal of Pharmaceutics and Biopharmaceutics 72 (2009) 62–68

Contents lists available at ScienceDirect

European Journal of Pharmaceutics and Biopharmaceutics

journal homepage: www.elsevier.com/locate/ejpb

Research paper

Dye diffusion from microcapsules with different shell thickness into mammalian skin

Huai Nyin Yow [a], Xiao Wu [b], Alexander F. Routh [a,*], Richard H. Guy [b]

[a] Department of Chemical Engineering and Biotechnology, BP Institute, University of Cambridge, Cambridge, UK
[b] Department of Pharmacy and Pharmacology, University of Bath, Claverton Down, Bath, UK

ARTICLE INFO

Article history:
Received 15 May 2008
Accepted in revised form 10 November 2008
Available online 27 November 2008

Keywords:
Encapsulation
Skin diffusion
Microcapsules

ABSTRACT

Oil-in-water microcapsules with varying shell thicknesses were fabricated via a coacervation technique, whereby evaporation of volatile solvents induced the shell-forming polymer to precipitate, phase separate and migrate to the oil/water interface to form microcapsules. These microcapsules encapsulated a lipophilic dye within their cores and were applied topically onto porcine skin for 6 h. Results indicated that the dye preferentially accumulated within the skin furrows and hair follicles, though the dye did not penetrate beyond the stratum corneum. A model estimates the diffusion coefficients of dye through the microcapsule shell and within the skin to be approximately 10^{-18} and 10^{-16} m^2 s^{-1}, respectively.

1. Introduction

In the past 35 years, microcapsules have found broad applications in many drug and vitamin products [1,2], cosmetics, personal care items [3,4] and food and beverages [5,6]. Release mechanisms of the encapsulated ingredients include rupture by stress/pressure, shell dissolution [7], shell permeation [8] and responsive shell swelling [9–12]. This variety provides a range of release profiles, for example, shell breakage and/or dissolution offers immediate release, while permeable and/or swellable shells are more useful for gradual, targeted release.

Despite their widespread use, however, safety concerns remain about the fate of microstructures in the human organism [13], an issue which has achieved even greater prominence with the advent of 'nanotechnology' in recent years. The motivation for this work lies in the investigation of percutaneous transport of an encapsulated ingredient into the skin from permeable microcapsules with varying shell thicknesses. This, coupled to a simple model for the diffusion profiles, crucially allows the understanding of individual control parameters for the 'active' ingredient movement within each environment (polymeric shell and skin). Hence, in this paper, polystyrene microcapsules (700–900 nm) had been used to encapsulate a model, 'active' ingredient (Nile Red dye) and then applied topically on porcine skin. Subsequently, the release and penetration of the 'active' were investigated and the results were modelled.

Microcapsules were prepared using a previously reported coacervation method [14–16], whereby the shell-forming polymer and oil core are initially premixed in a volatile solvent, in which the polymer is soluble. The oil phase is then emulsified in an aqueous solution and the emulsification intensity determines the size of capsules formed. As the volatile solvent evaporates, the polymer precipitates from the oil phase. Given the right wetting conditions, the polymer will migrate to the water/oil interface and envelope the oil droplet to form a complete spherical shell. The final morphology of the particles is governed by the relative interfacial energies between the various phases [14].

Porcine skin has been used as a substitute for human skin, which closely resembles human skin in terms of epidermal thickness, lipid composition, permeability to diverse compounds and overall barrier function [17]. The latter is furnished by the stratum corneum, the thin (~10 μm) outermost layer of the skin. It has been described as a 'brick and mortar' structure [18], in which corneocytes are embedded in an intercellular lipid matrix composed of ceramides, free fatty acids and cholesterol.

2. Theory

2.1. Dye diffusion model

The polystyrene shells encapsulated Nile Red dye and hexadecane cores. As the formulation of microcapsules came into contact with the porcine skin, passive diffusion of dye from the oil core into the skin takes place over the duration of the application time. This dye diffusion process is described by Fick's second law of diffusion

$$\frac{\partial c}{\partial t} = D\frac{\partial^2 c}{\partial x^2}. \quad (1)$$

* Corresponding author. Department of Chemical Engineering and Biotechnology, BP Institute, University of Cambridge, Cambridge, UK. Tel.: +44 1223 765718.
E-mail address: afr10@cam.ac.uk (A.F. Routh).

0939-6411/$ - see front matter © 2008 Elsevier B.V. All rights reserved.
doi:10.1016/j.ejpb.2008.11.004

Notations

c	dye concentration within stratum corneum	t	formulation application time
C_{NR}	dye concentration within oil core	V_s	volume of microcapsule shell
D	diffusion coefficient through stratum corneum	V_t	total volume of one microcapsule
D_s	diffusion coefficient through microcapsule shell	ϕ_p	polymer fraction within non-volatile non-solvent oil
L	thickness of stratum corneum	x	distance into stratum corneum
L_s	thickness of microcapsule shell		
r	radius of microcapsule		

Fig. 1 presents the system schematically, with the microcapsule encapsulating the active (in this work, the Nile Red dye) at a concentration C_{NR}. The microcapsules have a shell thickness of L_s and diffusion of dye through the shell is characterised by a diffusion coefficient, D_s. The microcapsules are in contact with the stratum corneum, of thickness L. The Nile Red diffusion coefficient through the skin is D, and its concentration within the stratum corneum is represented by c and is a function of application time (t) and distance (x) into the stratum corneum.

The applicable boundary conditions are

(i) At $x = 0$, $\frac{\partial c}{\partial x} = 0$, which represents no flux of material at the inner surface of the skin.
(ii) At $x = L$, $\frac{D_s(C_{NR} - c)}{L_s} = D\frac{\partial c}{\partial x}$, which represents a balance between the amount of dye passing through the shell and that passing through the stratum corneum.

For ease of calculation, the concentration gradient, $(C_{NR} - c)$, is normalised by the Nile Red concentration in the oil core. The thickness of capsule shell is also normalised, in this case, by the thickness of the stratum corneum yielding the dimensionless parameters

$$\hat{c} = \frac{c}{C_{NR}} - 1 \quad \text{and} \quad \hat{x} = \frac{x}{L} \tag{2}$$

and the simplified form of Eq. (1)

$$\frac{\partial \hat{c}}{\partial t} = \frac{D}{L^2}\frac{\partial^2 \hat{c}}{\partial \hat{x}^2} \tag{3}$$

with revised boundary conditions

(i) At $\hat{x} = 0, \frac{\partial \hat{c}}{\partial \hat{x}} = 0$.
(ii) At $\hat{x} = 1, D\frac{\partial \hat{c}}{\partial \hat{x}} = -\frac{D_s L}{L_s}\hat{c}$.

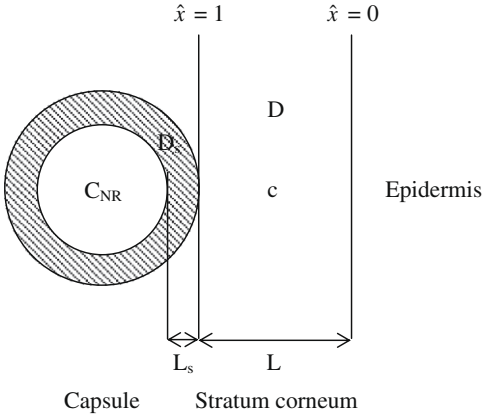

Fig. 1. Schematic diagram illustrating the basis of the mathematical model developed (not to scale).

Solution is obtained by separation of variables, resulting in an Eigenfunction series with the Eigenfunction, λ, given by the solution to

$$\lambda \tan \lambda = \frac{D_s L}{D L_s} \tag{4}$$

and the solution for concentration as follows

$$\hat{c} = \sum_{n=1}^{\infty} A_n \exp\left(-\frac{\lambda_n^2 Dt}{L^2}\right)\cos \lambda_n \hat{x} \tag{5}$$

with the values of A_n obtained from

$$A_n = -\frac{4 \sin \lambda_n}{2\lambda_n + \sin 2\lambda_n} \tag{6}$$

In summary, the diffusion of dye through the microcapsule shell into the stratum corneum is characterised by Eq. (5), with λ_n provided in Eq. (4) and the corresponding A_n calculated from Eq. (6), where $n = 1, 2, 3\ldots$

2.2. Solution when $C_{NR} \gg c$

When the 'active' concentration within the oil core, C_{NR}, is much greater than that within the stratum corneum, c (i.e., $C_{NR} \gg c$), then the concentration difference $(C_{NR} - c)$ dominates the passive diffusion process, which is no longer governed by the thickness of the shell.

Using Fig. 1 with the illustrated symbols and notations, together with Eq. (1) and the corresponding boundary conditions given before, and defining

$$\breve{c} = c \times L_s \quad \text{and} \quad \hat{x} = \frac{x}{L} \tag{7}$$

then

$$\frac{\partial \breve{c}}{\partial t} = \frac{D}{L^2}\frac{\partial^2 \breve{c}}{\partial \hat{x}^2} \tag{8}$$

and

(i) At $\hat{x} = 0, \frac{\partial \breve{c}}{\partial \hat{x}} = 0$.
(ii) At $\hat{x} = 1, \frac{D}{L}\frac{\partial \breve{c}}{\partial \hat{x}} = D_s C_{NR}\left(1 - \frac{c}{C_{NR}}\right)$.

However, since $C_{NR} \gg c$ or $c/C_{NR} \ll 1$, then the second boundary condition becomes

$$\frac{\partial \breve{c}}{\partial \hat{x}} = \frac{D_s L C_{NR}}{D} \tag{9}$$

which is independent of the capsule shell thickness, L_s.

Therefore, the solutions to Eq. (8) will be independent of shell thickness, L_s, and the data obtained from different microcapsules should then collapse onto a single profile, providing a simple proof that the dye diffusion through the stratum corneum follows simple Fickian diffusion.

3. Experimental

3.1. Materials

Polystyrene (melt index 14, MW ~225,000 g/mol, Aldrich, Dorset, UK) was used to form the microcapsule shells. Dichloromethane (99%, Acros Organics, Loughborough UK) was the volatile polymer solvent. *n*-Hexadecane (99%, Fisher Scientific, Loughborough, UK) was employed without purification as the non-volatile, non-solvent oil core. Acetone (>99%, Aldrich) was added to aid the emulsification process. Poly(vinyl alcohol) (96% hydrolysed – average MW 85,000–124,000 g/mol, Aldrich) was the external aqueous phase after dilution to 2% w/v solution with MilliQ water (18.2 MΩ cm). Nile Red (Aldrich), a fluorescent dye, was the encapsulated, lipophilic 'active'. Acetonitrile (HPLC grade, Aldrich) was the solvent used in the high-performance liquid chromatography (HPLC) assay of Nile Red (see below).

Anhydrous sodium phosphate dibasic (Acros Organics), potassium dihydrogen phosphate monobasic (Acros Organics) and sodium chloride (Acros Organics) were used to make phosphate-buffer solutions. Phosphoric acid (85% in solution, Acros Organics) was added for pH adjustment. Porcine skin was obtained from four 1-year-old pigs (two female and two male) from a local slaughterhouse. Tissue was dermatomed to a nominal depth of 750 μm, then cut into 4 cm × 6 cm pieces. The skin samples were washed under cold running water, dried, and sealed in plastic bags at −20 °C until used.

3.2. Methods

3.2.1. Fabrication of polystyrene microcapsules with encapsulated dye

Polystyrene microcapsules were made using a coacervation technique; the precipitated polymer induced by internal phase separation enveloped the oil core to form a complete shell [14–16,19]. Nile Red (1.6 mg) was first pre-dissolved in hexadecane (24 g) and acetone (6.2 g). The presence of acetone facilitated dissolution without causing phase separation from hexadecane. This mixture was then separated into four identical batches.

Next, polystyrene (3.2–16 g) was dissolved in dichloromethane (110.2 g) and a batch of the Nile Red containing oil phase was added. Additional acetone (4.65 g) was introduced to aid the subsequent emulsification process. Meanwhile, 2% w/v poly(vinyl alcohol) solution (125 mL) was poured into a 400-mL beaker and thermostated at 20 °C.

With the aqueous phase being stirred at approximately 9200 rpm, the oil phase was gradually added over ~1 min to form an oil-in-water emulsion. Stirring was continued for 1 h. Subsequently, the emulsion was heated, with gentle stirring, from 20 to 65 °C over 20 min and was then maintained at this elevated temperature for a further 40 min. The temperature was then reduced to 40 °C and held for 4 h. Finally, the emulsion was left overnight in a fume cupboard at atmospheric conditions, again with gentle stirring. This ensured that all the dichloromethane and acetone had evaporated and allowed for complete polystyrene shell formation. The formed microcapsules were then placed in sealed containers and kept in the dark until use.

3.2.2. Characterisation of polystyrene microcapsules

The microcapsules were characterised by scanning electron microscopy (SEM). A JEOL-6340F Field Emission Gun Scanning Electron Microscope was used to image the morphology of the microcapsules at an accelerating voltage of 5 kV. A drop of the microcapsule suspension was air-dried on a stainless steel SEM stub overnight. The sample was then platinum-coated using an Emitech K575 sputter coater. This was carried out under argon at 1×10^{-3} mbar and 40 mA for 1 min.

The microcapsule diameters were measured by dynamic light scattering (Brookhaven ZetaPlus, Brookhaven Instruments Corporation, Holtsville, NY, USA). A drop of the microcapsule dispersion (approximately 0.1 mL) was placed in a disposable plastic cell and diluted to 3 mL. The effective diameters deduced were accurate to ±1%, with an average of 10 measurements taken.

3.2.3. Dye diffusion study

Before the experiment, the skin was fully defrosted and any visible hairs were trimmed as close as possible to the surface. Each piece of skin was cut in half, one part being used for the Nile Red diffusion experiment, the other reserved for the measurement of stratum corneum thickness (see below).

The former piece of skin was clamped between the donor and receptor compartments of a vertical Franz diffusion cell. The receptor compartment was filled with phosphate buffer solution. The donor solution was 3 mL of a polystyrene microcapsule formulation and was covered with Parafilm to prevent evaporation. Replicate cells ($n = 3$) were positioned on a Skin Permeation System (Model LG-1083, Laboratory Glass Apparatus Inc, Berkeley, CA, USA), which allowed magnetic stirring of the receptor phases and provided a means to thermostat the cells at 37 °C. Diffusion was allowed to proceed for 6 h, at which point the experiment was terminated, the skin removed and gently washed three times with phosphate buffer solution, and patted dry with paper towel.

Subsequently, the depth of Nile Red penetration into the stratum corneum of porcine skin was assessed using a validated tape-stripping procedure [20]. Briefly, twenty 2.7 cm × 2.7 cm square tapes were first cut from transparent Scotch adhesive book tape 845. Each tape was weighed pre- and post-skin stripping. A circular template with a 2-cm diameter hole was prepared and secured onto the treated skin. The stratum corneum was then stripped 20 times with the pre-weighed tapes. After, each tape was rolled and placed in 1 mL acetonitrile in a 2-mL glass vial. The vials were capped and shaken overnight. The next day, the samples were filtered (Whatman PTFE filters, 0.45 μm, Florham Park, NJ, USA) into HPLC vials. The experimental solutions, together with known concentration standards of Nile Red, were assayed by HPLC.

3.2.4. High-performance liquid chromatography assay

Nile Red was quantified by HPLC with fluorescence detection. The chromatographic system (Dionex, Sunnydale, CA, USA) was equipped with a RF 2000 fluorescence detector and a reversed-phase column (25 cm × 4.6 mm internal diameter, KYA Tech, Tokyo, Japan). The system was set at 559 and 630 nm for excitation and emission wavelengths, respectively. The mobile phase was acetonitrile–water (80:20) with a flow rate of 1 mL/min. Each injection utilised 200 μL of solution maintained at 25 °C. The Nile Red retention time was 12.6 min. The limits of detection and quantitation were 0.3 and 1.1 ng/mL, respectively.

3.2.5. Stratum corneum thickness determination

The second half of each skin section was used for measurement of stratum corneum thickness using a previously published method [21]. Stratum corneum removal using pre-weighed tape-strips was again employed, having delimited a 2-cm diameter area of skin with a circular template. Prior to the first strip and following the removal of each layer, the passive transepidermal water loss (TEWL) across the skin was measured with an Aquaflux device (Biox Systems Ltd., London, UK) specifically designed for this purpose. Stripping was continued until TEWL reached 80 g m^{-2} h^{-1} [21]. Then, the tapes were reweighed to determine the amount (and, hence, the thickness) of stratum corneum removed on each

tape-strip. The reciprocal of TEWL was plotted against the cumulative thickness of stratum corneum removed and the resulting linear regression was extrapolated to $TEWL^{-1} = 0$ to yield the total stratum corneum thickness as the intercept on the x-axis.

3.2.6. Laser scanning confocal microscopy

After 6 h of exposure to the Nile Red microcapsule formulation, the skin was cleaned and then examined by laser scanning confocal microscopy (LSM 510 Meta, Carl Zeiss, Jena, Germany). A HeNe laser was used to excite Nile Red at 543 nm. The skin was then inspected under 10×, 20× and 63× objectives. Confocal images were recorded and edited with LSM Image Browser software (Carl Zeiss, Release 4.0).

4. Results and discussion

4.1. Polystyrene microcapsules

Fig. 2 is a SEM image of polystyrene microcapsules encapsulating Nile Red. The capsules are spherical and range in size from 500 nm to 1 μm. This was confirmed quantitatively by dynamic light scattering, which gave an average effective diameter of 750 nm. Some microcapsules appeared to have a hole within their shells, and these structures have been termed "colloidal buckets". It is believed that the formation of these structures (which will be discussed in a separate article) is triggered by the presence of excess dye. As most of the particles formed did not display this feature, the analysis of the results assumed a continuous shell.

Five sets of polystyrene microcapsules were fabricated with varying shell thickness. This was achieved either by varying the amount of polystyrene or by decreasing the hexadecane content. The crucial element is the volume ratio of the shell-forming polymer to the non-volatile oil. This ratio governs the total surface area that the polymer must cover to form a complete shell and, in turn, for a given capsule diameter, determines the thickness of the shell that the precipitating polymer can produce.

To calculate the shell thickness, it is assumed that volume is conserved [14]. For a capsule of radius, r, with shell thickness, L_s, the ratio of volume occupied by the shell, V_s, to the total volume of the capsule, V_t, is

$$\frac{V_s}{V_t} = \frac{r^3 - (r - L_s)^3}{r^3} \tag{10}$$

This ratio equals the volume fraction of polystyrene (ϕ_p) within the non-volatile non-solvent oil. In this study, the oil phase is hexadecane. Hence, Eq. (10) can be rearranged as

$$\frac{L_s}{r} = 1 - (1 - \phi_p)^{1/3} \tag{11}$$

Hence, as ϕ_p is known and the radius of the microcapsules is determined by dynamic light scattering, the shell thickness, L_s, can be calculated. The results for the different microcapsules are in Table 1. For the first, second and fourth series, the average capsule radius was 431 ± 12 nm and, with a threefold increase in polymer content, L_s approximately doubled; for the third and fifth sets, reducing the amount of hexadecane by a factor of 2 resulted in a 1.5-fold increase in L_s. In summary, therefore, it proved possible to obtain a range of microcapsules with varying shell thickness to be examined in subsequent experiments.

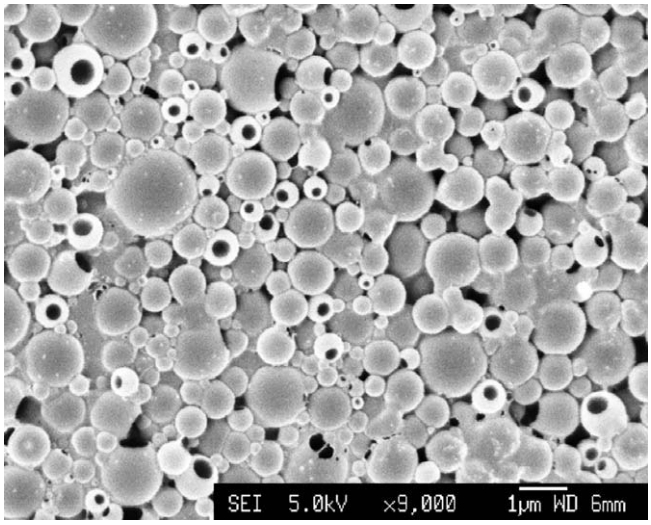

Fig. 2. Scanning electron microscopy image of polystyrene microcapsules.

Table 1
Properties of the various polystyrene microcapsules investigated.

Set	Polystyrene content (cm^3)	Hexadecane content (cm^3)	Polymer fraction, ϕ_p (%)	Capsule radius,[a] r (nm)	Shell thickness, L_s (nm)
1	3.1	8.7	26	425	40
2	5.9	8.7	40	445	70
3	11.9	10.3	54	360	82
4	9.0	8.7	51	425	89
5	11.8	5.0	70	360	120

[a] Measured by dynamic light scattering.

4.2. Confocal microscope imaging of skin

Fig. 3 shows that Nile Red had accumulated in the dermatoglyphics, or furrows, of the skin (Fig. 3a) and in and around the hair follicle openings (Fig. 3b). It is perhaps not surprising that this lipophilic fluorophore showed a predilection for these lipid-rich sites on or near the skin surface, and the data are consistent with earlier observations [22]. However, these skin appendages cover only 0.1% of the total skin surface, hence the contribution of this to percutaneous transport is considered minimal [23]. It is generally the intercellular lipid matrix that is the main barrier to percutaneous transport.

4.3. Skin penetration of Nile Red

The thickness of the stratum corneum of 10 pieces of porcine skin was determined via measurements of TEWL. Examples of the data obtained are shown in Fig. 4. The x-axis intercept gives the total thickness of the stratum corneum. Therefore, the average (±SD) stratum corneum thickness is 10 ± 2 μm. With this information, it was possible to display all Nile Red concentration profiles across the barrier as a function of normalised position (from 0 at the skin surface to 1 at the interface with the underlying viable tissue). The Nile Red concentrations were obtained by dividing the Nile Red amount, as detected by HPLC, by the volume of stratum corneum, assuming a density of 1 g cm^{-3} [24].

The Nile Red concentration profiles observed as a function of microcapsule shell thickness are illustrated in Fig. 5. The diffusion of dye into the deeper regions of the stratum corneum indicates that it has been released from the microparticles, the size of which are clearly too large to cross an intact cutaneous barrier [25]. Apparent from the data, however, is that a gradual increase in the microcapsule shell thickness resulted in a decrease in the amount of Nile Red taken up into the stratum corneum. This has been confirmed quantitatively by integration of the area under the concentration profiles to give the calculated total amount of

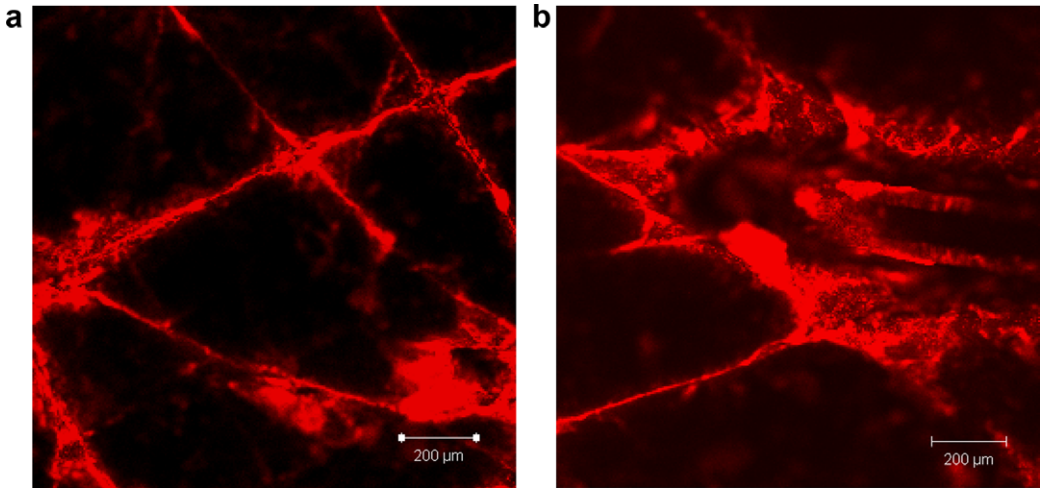

Fig. 3. Laser scanning confocal microscopy images showing Nile Red deposition (a) in skin furrows and (b) in and around a hair follicle.

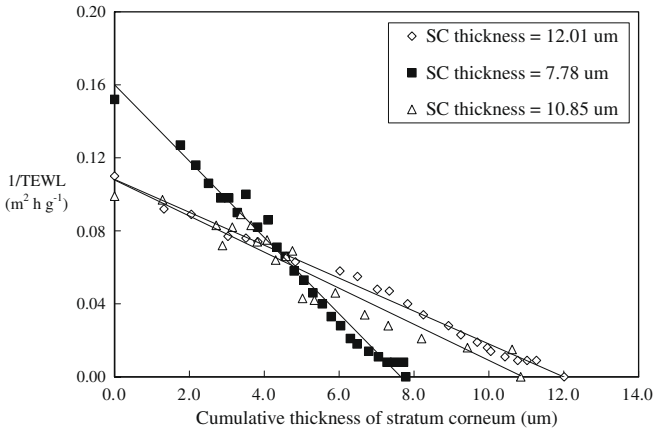

Fig. 4. Example TEWL results enabling stratum corneum thickness determination.

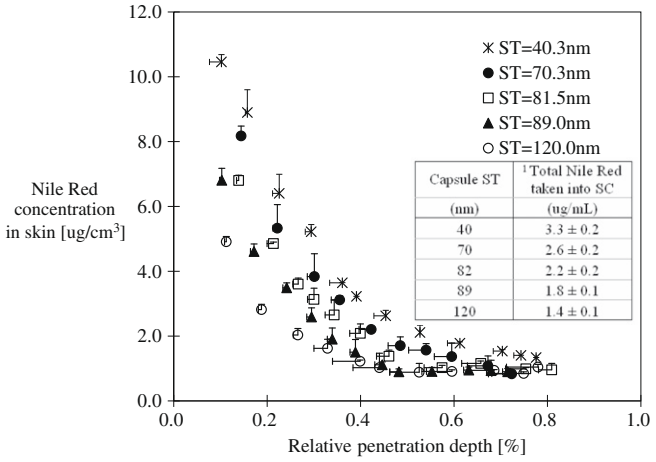

Capsule ST (nm)	[1]Total Nile Red taken into SC (ug/mL)
40	3.3 ± 0.2
70	2.6 ± 0.2
82	2.2 ± 0.2
89	1.8 ± 0.1
120	1.4 ± 0.1

Fig. 5. Nile Red concentration profiles across the stratum corneum (mean ± SD; $n = 3$) as a function of the relative depth of penetration into the barrier following a 6-h application of five formulations of microcapsules of different shell thickness (ST). [1]Determined by integration of the area under the curves in this figure.

Nile Red uptake as a function of microcapsule thickness (inset table in Fig. 5). These results suggest a means whereby the uptake of an 'active' ingredient into the skin may be manipulated by judicious design of the formulation employed.

4.4. Model fitting

The Nile Red concentration profiles across the stratum corneum were fitted to the theoretical model, using 10 terms in the Eigenfunction expansion to ensure convergence. The best fit to the data (Fig. 6a) were obtained with $D = 5\times10^{-16}\ m^2\ s^{-1}$ and $D_s = 1.5 \times 10^{-18}\ m^2\ s^{-1}$. To the authors' best knowledge, no coefficient data had been quoted for diffusion of Nile Red dye in pig skin or polystyrene shell. Comparing with similar release studies, the proposed coefficients were comparable to literature; 10^{-15} to $10^{-16}\ m^2\ s^{-1}$ for D [26,27] and 10^{-16} to $10^{-21}\ m^2\ s^{-1}$ for D_s [8,28,29]. The diffusion of an active is generally governed by its size, solubility in the diffusion medium and nature of the diffusion medium. The sensitivity of the fitting to the values of the proposed diffusivities is illustrated in Fig. 6b and c. Predictably, as D is increased from 10^{-17} to $10^{-14}\ m^2\ s^{-1}$, the 'active' distributes further into the barrier and the profile becomes progressively less steep (Fig. 6b). On the other hand, as D_s is increased from 10^{-20} to $10^{-17}\ m^2\ s^{-1}$, the total amount of 'active' in the stratum corneum increases progressively as its release from the microcapsules becomes faster (Fig. 6c). Overall, therefore, diffusivity in the shell determines the absolute quantity of 'active' transferred into the stratum corneum, while its diffusivity in this membrane controls the depth of penetration into the skin.

The Nile Red profiles in Fig. 6a indicate that the concentration of 'active' in the oil core is much greater than that achieved in the stratum corneum. The approximate solution to the diffusion equation when $C_{NR} \gg c$ can be applied, and the theoretical prediction that the behaviour of $(c \times L_s)$, as a function of penetration depth into the stratum corneum, is independent of microcapsule shell thickness may be examined. This test is undertaken as shown in Fig. 7, and a collapse of the data onto a single profile is observed. Hence, this confirms that the dye diffusion process into the porcine skin is governed by Fickian diffusion.

5. Conclusions

A range of polystyrene microcapsules, encapsulating Nile Red in hexadecane core, were prepared and examined for their ability to deliver a model 'active' substance to the outer layers of mammalian skin. Increasing shell thickness reduced the rate and extent of 'active' transfer into the outermost, and least permeable, layer of skin, the stratum corneum. The concentration profiles were suc-

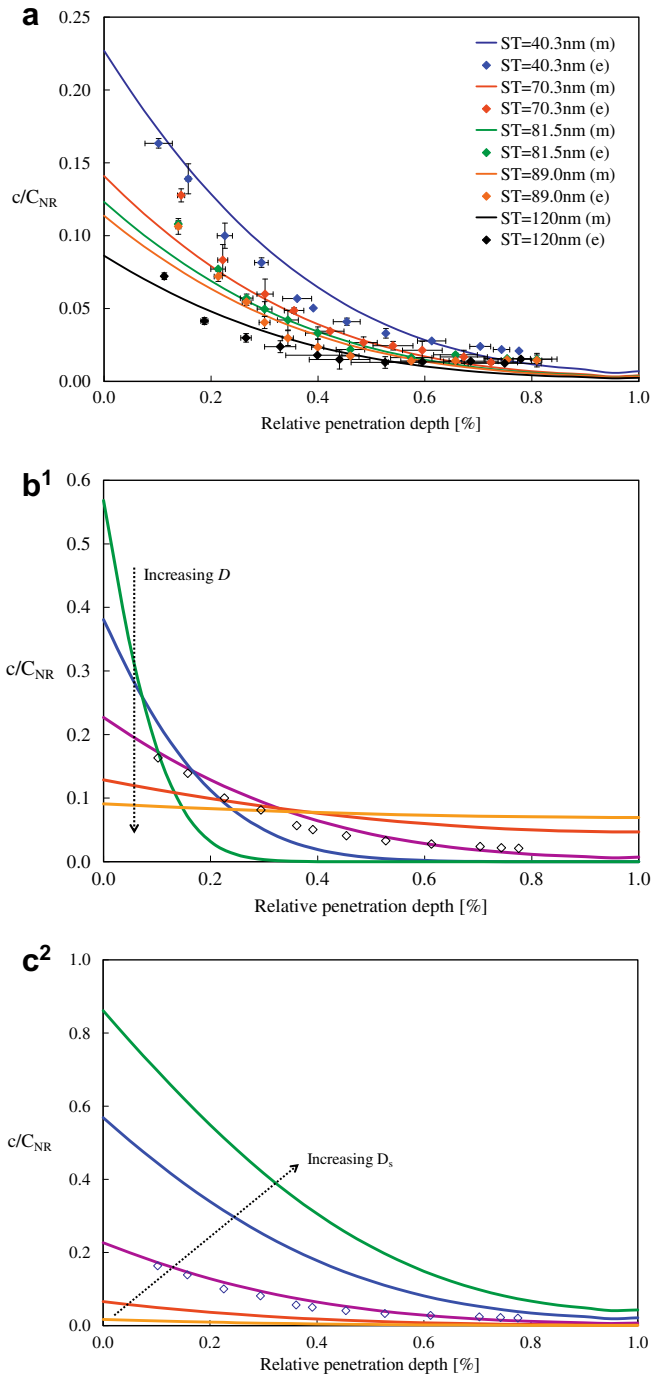

Fig. 6. (a) Comparison of normalised Nile Red concentration (c/C_{NR}) profiles (mean ± SD; $n = 3$) across the stratum corneum with the theoretical predictions (continuous lines) of the model for 'active' delivery from microcapsules of different shell thickness (ST), with subsequent model predictions of the normalised Nile Red concentration (c/C_{NR}) profile for various values of diffusion coefficient of the 'active' (b) across the stratum corneum, D, and (c) through the polymeric microcapsule shell, D_s. [1]The data points shown are for Nile Red delivered from a formulation containing microcapsules of shell thickness 40 nm and having $D = 5 \times 10^{-16}$ m^2 s^{-1}. [2]The data points shown are for Nile Red delivered from a formulation containing microcapsules of shell thickness 40 nm with $Ds = 1.5 \times 10^{-18}$ m^2 s^{-1}.

cessfully simulated with a diffusion model, which took into account the active's diffusivities in the stratum corneum and in the polymeric shell. The results suggested that the approach might be useful for the design and optimisation of consumer-health formulations for diverse applications.

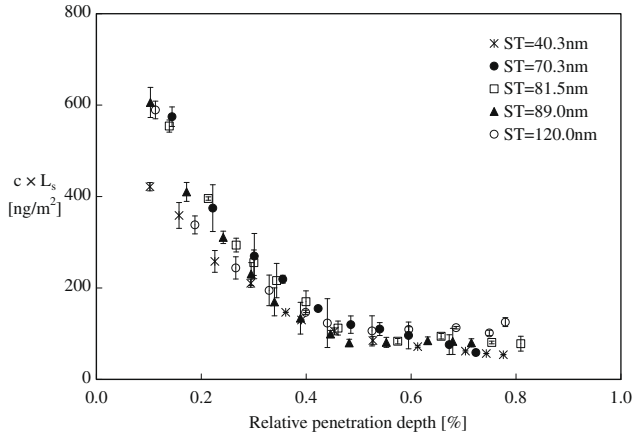

Fig. 7. Predicted collapse of concentration profile data in Fig. 5 to an essentially common profile when $C_{NR} \gg c$ (the case for these experiments) [data shown are mean ± SD for $n = 3$].

Acknowledgements

This research was funded by the European Union, via an integrated project entitled NAPOLEON (NAnostructured waterborne POLymEr films with OutstaNding properties). Huai Nyin Yow and Xiao Wu are both the recipients of Overseas Research Studentship awards.

References

[1] Frost, Sullivan, Microencapsulated pharmaceuticals to thrive, in: Laboratory Talk, Letchworth. Available from: <http://www. laboratorytalk.com/news/fro/fro128.html>, 2002.
[2] W. Meier, Polymer nanocapsules, Chemical Society Reviews 29 (5) (2000) 295–303.
[3] Unilever UK, Extra Protection When You Need It. Available from: <http://www.unilever.co.uk/ourvalues/sciandtech/science_behind_vitality/extra_protection.asp>, 2007.
[4] Y. Ueda, A. Segawa, M. Yoshioka, The characteristics of a microcapsule with an entirely new wall material, 'silicone–resin–polypeptide', and its application, International Journal of Cosmetic Science 26 (2004) 215.
[5] J. Wozniak, Eat them ALIVE, in: Nutra Solutions. Available from: <http://www.nutrasolutions.com/CDA/ArticleInformation/features/BNP__Features__Item/0,1269,113054,00.html>, July 2002.
[6] J. Franjione, N. Vasishtha, The art and science of microencapsulation, Technology Today (1995).
[7] B.F. Gibbs, S. Kermasha, I. Alli, C.N. Mulligan, Encapsulation in the food industry: a review, International Journal of Food Sciences and Nutrition 50 (1999) 213–224.
[8] M.S. Romero-Cano, B. Vincent, Controlled release of 4-nitroanisole from poly(lactic acid) nanoparticles, Journal of Controlled Release 82 (1) (2002) 127–135.
[9] M. Sauer, D. Streich, W. Meier, pH-sensitive nanocontainers, Advanced Materials 13 (2001) 1649–1651.
[10] G. Ibarz, L. Dähne, E. Donath, H. Möhwald, Smart micro- and nanocontainers for storage, transport, and release, Advanced Materials 13 (2001) 1324–1327.
[11] A. Shulkin, H.D.H. Stover, Photostimulated phase separation encapsulation, Macromolecules 36 (2003) 9836–9839.
[12] L. Zha, Y. Zhang, W. Yang, S. Fu, Monodisperse temperature-sensitive microcontainers, Advanced Materials 14 (2002) 1090–1092.
[13] E. Strickland, Nice nanostuff, but is it safe? in: East Bay Express. Emeryville, USA. Available from: http://www.eastbayexpress.com/2006-01-25/news/nice-nanostuff-but-is-it-safe/, January 2006.
[14] A. Loxley, B. Vincent, Preparation of poly(methylmethacrylate) microcapsules with liquid cores, Journal of Colloid and Interface Science 208 (1998) 49–62.
[15] P.J. Dowding, R. Atkin, B. Vincent, P. Bouillot, Oil core–polymer shell microcapsules prepared by internal phase separation from emulsion droplets. I: Characterization and release rates for microcapsules with polystyrene shells, Langmuir 20 (2004) 11374–11379.
[16] P.J. Dowding, R. Atkin, B. Vincent, P. Bouillot, Oil core/polymer shell microcapsules by internal phase separation from emulsion droplets. II: Controlling the release profile of active molecules, Langmuir 21 (12) (2005) 5278–5284.
[17] N. Sekkat, Y.N. Kalia, R.H. Guy, Biophysical study of porcine ear skin in vitro and its comparison to human skin in vivo, Journal of Pharmaceutical Science 91 (2002) 2376–2381.

[18] P.M. Elias, Lipids and the epidermal permeability barrier, Archives of Dermatological Research 270 (1981) 95–117.
[19] H.N. Yow, A.F. Routh, Formation of liquid core–polymer shell microcapsules, Soft Matter 2 (2006) 940–949.
[20] V.P. Shah, Topical Dermatological Drug Product NDAs and ANDAs – In Vivo Bioavailability, Bioequivalence, In Vitro Release and Associated Studies, US Department of Health and Human Services, Rockville, 1998. pp. 1–9.
[21] Y.N. Kalia, F. Pirot, R.H. Guy, Homogeneous transport in a heterogeneous membrane: water diffusion across human stratum corneum in vivo, Biophysical Journal 71 (1996) 2692–2700.
[22] R. Alvarez-Roman, A. Naik, Y.N. Kalia, R.H. Guy, H. Fessi, Skin penetration, distribution of polymeric, nanoparticles, Journal of Controlled Release 99 (2004) 53–62.
[23] K. Moser, K. Kriwet, A. Naik, Y.N. Kalia, R.H. Guy, Passive skin penetration enhancement and its quantification in vitro, European Journal of Pharmaceutics and Biopharmaceutics 52 (2001) 103–112.
[24] R.L. Anderson, J.M. Cassidy, Variations in physical dimensions and chemical composition of human stratum corneum, Journal of Investigative Dermatology 61 (1973) 30–32.
[25] A. Rolland, N. Wagner, A. Chatelus, B. Shroot, H. Schaefer, Site-specific drug delivery to pilosebaceous structures using polymeric microspheres, Pharmaceutical Research 10 (1993) 1738–1744.
[26] C. Herkenne, A. Naik, Y.N. Kalia, J. Hadgraft, R.H. Guy, Ibuprofen transport into and through skin from topical formulations: in vitro-in vivo comparison, Journal of Investigative Dermatology 127 (2006) 135–142.
[27] K. Moser, K. Kriwet, C. Froehlich, Y. Kalia, R. Guy, Supersaturation: enhancement of skin penetration and permeation of a lipophilic drug, Pharmaceutical Research 18 (2001) 1006–1011.
[28] A. Choucair, P.S. Lim, A. Eisenberg, Active Loading and Tunable Release of Doxorubicin from Block Copolymer Vesicles, Langmuir 21 (2005) 9308–9313.
[29] N. Muro-Sune, R. Gani, G. Bell, I. Shirley, Predictive property models for use in design of controlled release of pesticides, Fluid Phase Equilibria 228–229 (2005) 127–133.